Alternative Membrane Protein Conformations in Alcohols†

D. E. Otzen,* P. Sehgal, and L. W. Nesgaard

Department of Life Sciences, Aalborg University, Sohngaardsholmsvej 49, DK-9000 Aalborg, Denmark

Received January 16, 2007; Revised Manuscript Received February 19, 2007

ABSTRACT: Alcohols modulate the oligomerization of membrane proteins in lipid bilayers. This can occur indirectly by redistributing lateral membrane pressure in a manner which correlates with alcohol hydrophobicity. Here we investigate the direct impact of different alcohol−water mixtures on membrane protein stability and solubility, using the two detergent-solubilized α-helical membrane proteins DsbB and NhaA. Both proteins precipitate extensively at intermediate concentrations of alcohols, forming states with extensive (40−60%) *β*-sheet structure and affinity for the fibril-specific dye thioflavin T, although atomic force microscopy images reveal layer-like and spherical deposits, possibly early stages in a fibrillation process trapped by strong hydrophobic contacts. At higher alcohol concentrations, both DsbB and NhaA are resolubilized and form non-native structures with increased (DsbB) or decreased (NhaA) helicity compared to the native state. The alternative conformational states cannot be returned to the functional native state upon dilution of alcohol. The efficiency of precipitation and the degree to which DsbB is destabilized at low alcohol concentrations show the same correlation with alcohol hydrophobicity. Thus, in addition to their effect on the membrane, alcohols perturb membrane proteins directly by solvating the hydrophobic regions of the protein. At intermediate concentrations, this perturbation exposes hydrophobic segments but does not provide sufficient solvation to avoid intermolecular association. Resolubilization requires a reduction in the relative dielectric constant below 65 in conjunction with specific properties of the individual alcohols. We conclude that alcohols provide access to a diversity of conformations for membrane proteins but are not a priori suitable for solution studies requiring reversible denaturation of monomeric proteins.

To remain soluble in the native state, membrane proteins (MPs)[1] need an amphiphilic environment, which can be provided by detergents or lipids. α-Helical MPs typically contain long consecutive sequences of hydrophobic amino acids in the transmembrane segments that allow the helices to dock against each other, stabilized through van der Waals interactions (*1*−*3*). *β*-Barrel MPs are made up of alternating hydrophilic−hydrophobic sequences that alternatively point into the protein interior and out toward the hydrophobic environment (*4*). As a consequence, it is actually possible to solubilize *β*-barrel membrane proteins in high concentrations of chemical denaturants such as guanidinium chloride and urea (*5*−*7*), where they remain in an extensively unfolded state. In contrast, α-helical MPs generally resist this treatment and are most commonly denatured in SDS (*8*−*11*), in which they retain significant amounts of residual helical structure. Thus refolding of *β*-barrel MPs can be followed by diluting the protein from high concentrations of denaturant into lipids or detergents (*6*), whereas α-helical MPs are typically refolded from SDS. The SDS-denatured state of many water-soluble proteins has been the subject of numerous structural studies (*12*−*15*) and appears to consist of isolated detergent-decorated helices joined by more flexible regions. A quantitative way to reversibly denature membrane proteins is to add increasing amounts of SDS in the presence of a constant concentration of a nonionic detergent such as dodecyl maltoside (DM) (*9*, *10*). There appears to be an empirical linear relationship between the SDS mole fraction and the log of the refolding and unfolding rates (*11*, *16*). This relationship also extends to thermal stability, provided account is taken of the micellar rather than bulk composition of detergent (*17*).

The SDS-denatured state retains significant residual structure (*11*, *18*). This may be analogous to the structure of nascent membrane proteins prior to lipid insertion (*19*). Nevertheless, recent reports indicating that this state may have native-like compaction (*20*) have led to the suggestion that the action of SDS may just as well be modeled by simple ligand binding rather than unfolding (*21*). This makes it relevant to look for alternative means of denaturation of membrane proteins.

One possibility is provided by alcohols, which are amphiphilic and contain a hydrophilic headgroup as well as a hydrophobic segment of varying lengths. Alcohols' denaturing action toward soluble proteins (*22*, *23*) is related to their reduction of the relative solvent dielectric constant ϵ_r, which

† D.E.O. is supported by the Danish Research Foundation (CureND) and the Villum Kann Rasmussen Foundation (BioNET). Part of this work was funded by a Visiting Scientist grant to D.E.O. from Osaka City University. P.S. was supported by the Innovation Consortium BIOPRO through a grant from the Danish Ministry of Science, Technology, and Innovation.

* To whom correspondence should be addressed. E-mail: dao@bio.aau.dk.

[1] Abbreviations: DM, dodecyl maltoside; DsbB, disulfide bond forming protein B; HFIP, hexafluoroisopropyl alcohol; iPrOH, 2-propanol; MPs, membrane proteins; NhaA, sodium hydrogen antiporter A; PrOH, *n*-propyl alcohol; TFE, trifluoroethanol.

10.1021/bi700091r CCC: $37.00
Published on Web 03/20/2007

may mimic conditions near the membrane surface (*24*−*26*). Increasing the alcohol concentration generally leads to a uniform increase in α-helicity (*24*, *27*−*30*). The reason for this is not entirely clear (*31*), although the lowered ϵ_r could conceivably strengthen internal hydrogen bonds which can be formed by isolated sequences in the α-helical conformation. However, trifluoroethanol can also induce the accumulation of *β*-sheet-rich aggregation-prone structures at intermediate (20−40%) concentrations and only induce α-helix structures at higher concentrations (*32*). As a further testimony to the versatility of alcoholic conformational switches, methanol but not longer chain alcohols has very recently been reported to induce *β*-sheet structure in an all-α-helix protein (*33*).

This then leads to the interesting question of whether alcohols can be used to reversibly denature membrane proteins for subsequent folding studies. The environment of the membrane protein stabilizing the native state can play a role in the protein's response to alcohols. Previous studies on the *Streptomyces lividans* potassium channel KcsA have shown that the stability of the tetramer in lipids is reduced by molar concentrations of alcohols in an indirect manner which can be related to their ability to alter the lateral membrane pressure and permeabilize the membrane (*34*, *35*). When KcsA is dissolved in detergents and TFE subsequently added, a partially and reversibly unfolded monomeric state is formed at intermediate TFE concentrations, but at higher TFE concentrations this state converts into an irreversibly denatured form (*36*). KcsA is an unusually stable α-helical MP which resists denaturation in SDS, making it possible to monitor its state of oligomerization on SDS−PAGE. Extrapolating on this, a recent study combines 2D gel electrophoresis with exposure to TFE or HFIP (hexafluoroisopropyl alcohol) to identify stable oligomeric membrane protein complexes, based on the criterion that they withstand exposure to SDS and only dissociate in alcohols (*37*). The quoted studies have focused on oligomeric proteins, and while many membrane proteins are found integrated into complexes, a significant number are monomeric. We would like to address the question how monomeric membrane proteins respond to alcohols, more specifically whether they can be unfolded to the same or greater extent by alcohols such as TFE and how reversible this behavior is.

Here we study the response of two α-helical membrane proteins to alcohols, namely, the four-transmembrane helix 176-residue disulfide-exchanging protein DsbB and the 388-residue sodium−hydrogen antiporter NhaA (*38*), both from the inner membrane of *Escherichia coli*. Both proteins can be unfolded in SDS (*39*), and in the case of DsbB, the protein can be reversibly folded into DM micelles as monitored by stopped-flow kinetics (*11*, *16*). We report that incubation with alcohols generally leads to precipitation at intermediate concentrations and the formation of a *β*-rich structure, which at higher concentrations is replaced by a soluble state with altered secondary structure. Both processes are irreversible, precluding the use of this approach for renaturation studies. The alcohols' ability to precipitate proteins, as well as their destabilizing properties at very low concentrations, is directly related to their hydrophobicity. We conclude that alcohols affect intrinsic membrane protein properties as well as exerting an effect via the membrane.

MATERIALS AND METHODS

DsbB (*11*), DsbA (*40*), NhaA (*39*), and AIDA (*41*) were purified as described. The buffer used in all experiments was 25 mM Tris, pH 8, and 0.1 M NaCl. This buffer, including different concentrations of detergent, was completely miscible with all of the alcohols analyzed in this study within the concentration range probed; turbidity was only observed above 40% (v/v) HFIP, 55% TFE, or 75% isopropyl alcohol. Note that the alcohols are expected to alter the pK_a of Tris by little more than 0.1 pH unit (cf. ref *42*). Given that DsbB retains full solubility in detergent over the pH range 3−10 and has unaltered stability over the pH range 8.5−6.5 (data not shown), these small changes in pK_a will not affect solubility or stability by themselves.

Equilibrium Denaturation Experiments. DsbB or NhaA (1.8 *μ*M) was incubated in buffer with 5 mM DM (unless otherwise indicated) and varying concentrations of alcohol in a total volume of 150 *μ*L. Following at least 30 min incubation at room temperature, the solution was centrifuged for 10 min at 14000 rpm and the fluorescence of the supernatant measured by excitation at 295 nm and emission between 310 and 400 nm with slit widths of 8 nm for both excitation and emission, using a LS55 fluorometer (Perkin-Elmer, Wellesley, MA). By using Trp fluorescence for these measurements, we were able to monitor conformational changes in addition to changes in solubility, as well as taking advantage of the superior sensitivity of fluorescence compared to absorbance.

Circular Dichroism. Typically 5 *μ*M protein was incubated in buffer with 5 mM DM and different concentrations of TFE. Circular dichroism spectra were recorded between 195 and 250 nm on a J-810 spectrometer (Jasco Spectroscopic Co. Ltd., Hachioji City, Japan) after at least 30 min of incubation using 1 mm cuvettes and an accumulation of three scans recorded at 20 nm/min with 1 nm bandwidth.

Thermal Scans by CD. These were performed with 5−10 *μ*M protein as described (*16*), following the change at ellipticity at 220 nm as a function of temperature in the presence of different concentrations of alcohols at a concentration range where precipitation did not occur to a significant extent.

Stopped-Flow Kinetics. DsbB in 5 mM DM and buffer was mixed 1:10 with TFE to a final concentration of 2.1 *μ*M DsbB, 5 mM DM, and 20% TFE on an SX18MV stopped-flow microanalyzer (Applied Photophysics, Surrey, Leatherhead, U.K.) at 25 °C. The reaction was followed by exciting at 280 nm and measuring emission above 320 nm using a glass cutoff filter.

DsbB Activity Assays. These were performed essentially as described (*40*, *43*). Typically, 1 *μ*M DsbB was mixed with 10 *μ*M reduced DsbA (from a 167 *μ*M stock where the Cys49−Cys52 bond was reduced in the presence of 10 mM DTT, desalted to remove excess DTT, and stored at −80 °C in 1 mM EDTA to avoid reoxidation) and 30 *μ*M decylubiquinone (from a 0.1 M stock in DMSO) in 300 mM NaCl and 50 mM sodium phosphate, pH 6. Emission was followed at 360 nm with excitation at 295 nm over 1 min. The linear decline in emission, caused by the formation of the Cys49−Cys52 disulfide bond in DsbA by the disulfide bonds in DsbB (*40*), was used as a quantitative measure of DsbB activity.

Thioflavin T Fluorescence. Following incubation with alcohols as described above, the solution was centrifuged for 10 min at 14000 rpm, the supernatant was removed by aspiration, and the pellet was resuspended in 120 μL of buffer containing 40 μM thioflavin T. Fluorescence was measured by excitation at 440 nm and emission at 385 nm using slits of 8 nm.

FTIR Data Acquisition. Spectra were recorded on a Bruker Tensor 27 infrared spectrometer (Bruker Optik GmbH, Ettlingen, Germany) with a Specac Golden Gate single-reflection ATR unit (Specac Ltd., Orpington, U.K.). Following incubation with alcohols as described above (40% for MeOH and EtOH, 30% for iPrOH, and 20% for TFE and PrOH), the solution was centrifuged for 10 min at 14000 rpm, the supernatant was removed by aspiration, and the pellet was resuspended in MilliQ water. Protein (2 μg) was dried under a gentle stream of nitrogen. Three independent samples were investigated (64 scans at 2 cm^{-1} resolution). One spectrum was collected for TFE. When necessary, we corrected for the presence of water vapor by subtracting a fresh water vapor spectrum. Peaks were assigned from the second derivative and deconvolution of spectra. The non-deconvoluted spectra were fitted using the Levenberg−Maquardt method to seven Lorentzian peaks, of which six were assigned to secondary structure elements and one low-intensity peak was assigned to contributions from side chains.

Atomic Force Microscopy. NhaA (5.4 μM) was incubated for 30 min in buffer with 2.8M TFE before centrifugation. The supernatant was removed by aspiration and the pellet washed twice in water. Protein (100 μL of 0.5 μM) was applied to freshly cleaved mica in a sample chamber, dried in an oven at 80 °C (typically 2−3 min), and removed from the oven as soon as the sample had dried. The elevated temperature was required to enable rapid drying and avoid leakage from the sample chamber. This handling does not appear to destroy, e.g., protein fibrils since it allows us to image fibrils of α-synuclein (data not shown). Samples were imaged in contact mode on a PicoSPMI apparatus (Molecular Imaging, Tempe, AZ) using silicon nitride cantilevers (BudgetSensors, Sofia, Bulgaria) with a force constant of 0.27 N/m.

RESULTS

Our initial interest was to analyze whether it was possible to reversibly and cooperatively denature DsbB in the fluorinated alcohol TFE to provide an alternative denaturation method. This would facilitate refolding experiments to compare with refolding from the SDS-denatured state, which is highly structured and contains approximately the same level of α-helicity as the state in DM (*11*).

DsbB Undergoes a Two-Step Irreversible Spectroscopic Change in the Presence of Increasing Concentrations of TFE, Involving Precipitation Followed by Resolubilization. A useful signature for cooperativity is a sigmoidal unfolding curve over a relatively narrow denaturant concentration interval [although sigmoidal unfolding curves can also be obtained from cooperatively and strongly binding ligands (*21*)]. We had failed to observe such cooperative unfolding of DsbB and NhaA when exposed to chemical denaturants in the presence of 5 mM DM. A linear decrease in the ratio of the Trp fluorescence emission at 335 and 350 nm was observed in response to increasing concentrations of guanidinium chloride (0−7 M) and urea (0−9 M) (data not shown). The ratio between these two wavelengths is often taken as a measure of the unfolding of a protein, since unfolding usually leads to a red shift of the emission spectrum (*44*).

We therefore turned to alcohols for denaturation. However, when DsbB was incubated with 0−55% TFE, we saw visible cloudiness over a relatively broad concentration interval. Upon centrifugation, sedimented pellets were observed predominantly around 10−35% TFE. The fluorescence of the supernatants showed a characteristic pattern: the intensity level remained unchanged up to 3% TFE, after which it plunged to around 25% of the original level as the TFE concentration was increased to 12%. The fluorescence remained at a low level up to around 30% TFE and then slowly increased to a level close to two-thirds of the original (Figure 1A). In parallel with this, the 335/350 nm emission ratio remained relatively constant around 1.1 to around 20% TFE, after which it fell to a new level around 0.95 where it remained as the TFE concentration increased to 50%.

The low concentration of DsbB made it unfeasible to use absorption at 280 nm as a measure of solubility. In order to obtain a more direct measure of the solubility of DsbB, we instead measured the ratio of the fluorescence of each sample before and after centrifugation and obtained a profile which was very similar to that of the absolute fluorescence spectrum, except that some lack of solubility was already observed at low concentrations of alcohol and the solubility at high alcohol concentrations reached close to 100% (Figure 1B). For the subsequent analysis, we will use the unprocessed fluorescence emission values for the supernatant rather than the ratio between the solution emission before and after centrifugation, due to problems with light scattering in the presence of suspended precipitates.

As might be expected, the presence of detergents has a significant impact on the ability of TFE to precipitate the protein. If the concentration of DM is decreased from 5 to 1 mM, the midpoint of precipitation is lowered by a factor of at least 2, while replacing DM with SDS increases the midpoint around 3-fold (data not shown). Nevertheless, the same profile involving precipitation and resolubilization was observed under all circumstances. In the following experiments, we kept the DM concentration constant at 5 mM to allow comparison between different alcohols.

CD spectra showed the expected typical α-helical structure in the absence of TFE, but at 20% TFE this is replaced by an essentially featureless spectrum due to extensive precipitation, while the spectrum in 50% TFE (where the solution is visibly clear and precipitation is insignificant; cf. Figure 1B) reveals a state with even higher α-helicity than the native state (insert to Figure 1A). Analysis of the CD spectra by the k2d algorithm (*45*) predicts an α-helix content of 59% (ca. 104 residues) in 0% TFE and 85% (ca. 150 residues) in the presence of 50% TFE, corresponding to an increase in helicity encompassing 46 residues. The transmembrane helices are modeled to consist of ca. 80 residues (*46*), accounting for the majority of the native state helicity. As the two cytoplasmic termini account for only around 25 residues, the increased helicity is most likely to reflect an increase in helicity in the two periplasmic loops as the protein goes from 0 to 50% TFE. We have in a recent thermody-

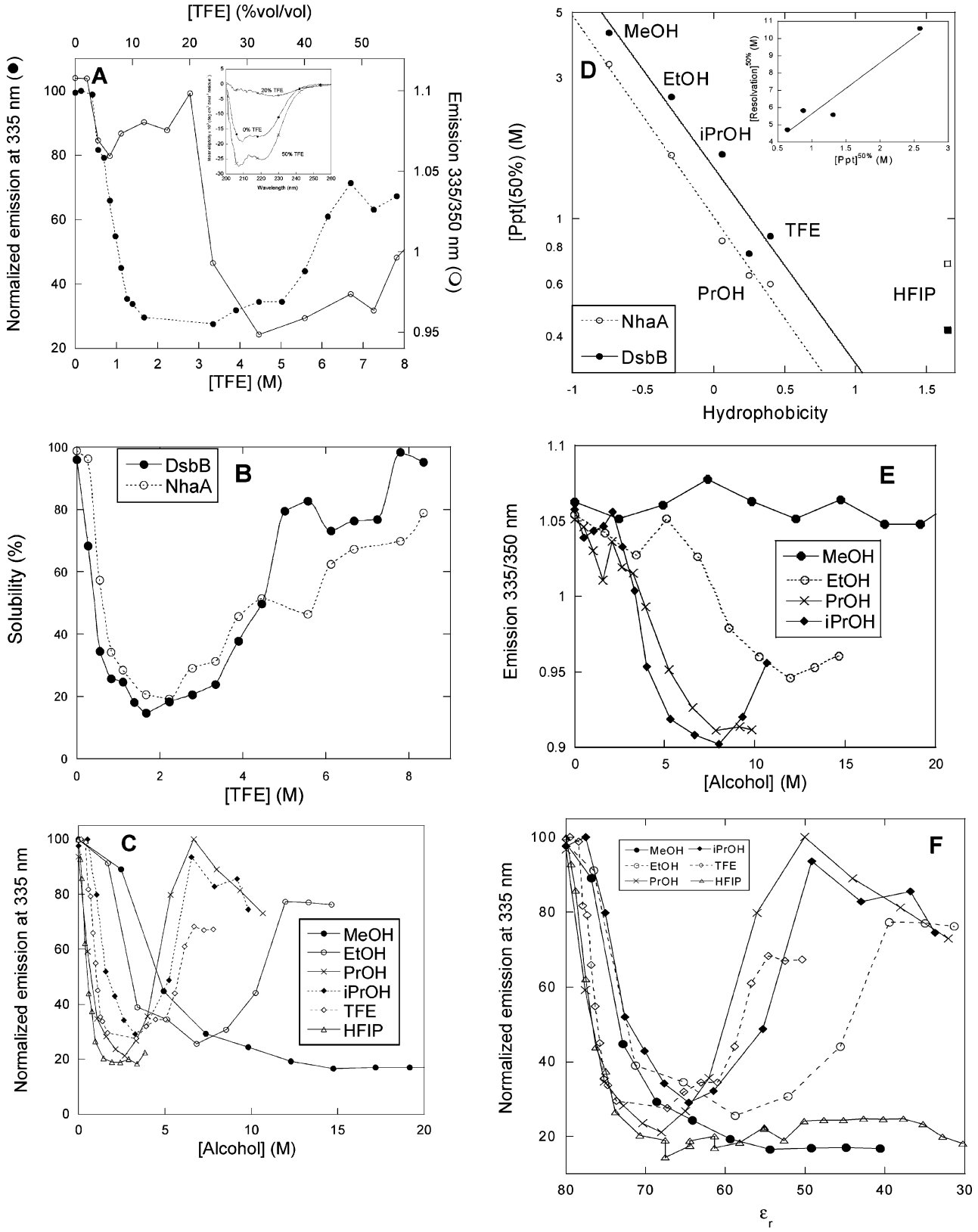

FIGURE 1: (A) Emission at 335 nm and the ratio of emission at 335 and 350 nm for DsbB incubated in different concentrations of TFE. After incubation in TFE for 30 min, the protein solution was spun down and the emission of the supernatant measured. Insert: Far-UV CD spectra of DsbB in the presence of 0−50% TFE. (B) Solubility of DsbB and NhaA at different TFE concentrations. The apparent fluorescence emission at 335 nm of the solution was measured before and after centrifugation. Light scattering due to aggregates contributes to emission before but not after centrifugation. (C) Emission of DsbB at 335 nm as a function of different alcohol concentrations. (D) Midpoint of precipitation $[Ppt]^{50\%}$ for DsbB and NhaA versus alcohol hydrophobicity plotted on a semilogarithmic scale (data for HFIP excluded from the fit). The slopes of the fitted straight lines are -1.53 ± 0.15 (DsbB) and -1.58 ± 0.05 (NhaA). Insert: $[Ppt]^{50\%}$ versus midpoint of resolubilization for DsbB. (E) Ratio of emission at 335 and 350 nm for DsbB incubated at different concentrations of alcohols. (F) Data in (C) plotted versus relative dielectric constant ϵ_r rather than alcohol concentration. Concentrations were converted to ϵ_r values based on data in ref *48*.

namic study concluded by indirect means that residues in the periplasmic loop in the native state are essentially unstructured (*16*), which ties in well with these observations.

The helically enriched species observed in 50% TFE represents a trapped state. If DsbB is transferred from 0 to 4.5% TFE, the protein retains around 80% of its biological activity, i.e., its ability to oxidize the periplasmic chaperone DsbA (see Materials and Methods). This agrees well with its solubility level in 4.5% TFE (Figure 1B). However, transfer from 50% to 4.5% TFE does not restore activity or the original low-TFE CD spectrum with reduced α-helix signals. As expected from the extensive precipitation, no activity was observed in 20% TFE.

On the basis of these observations, it appears that DsbB is not structurally perturbed by TFE until around 3% TFE, after which it starts to precipitate significantly. The soluble state present to a decreasing extent between 3% and 20% TFE appears to be native-like judged by the rather crude measure of the 335/350 nm ratio, but at higher TFE concentrations this is replaced by a state which according to both CD and 335/350 nm is soluble but irreversibly denatured to a non-native state, similar to the membrane protein KcsA (*36*).

Correlation between Hydrophobicity and Precipitation. The precipitation at intermediate TFE concentrations had not been observed for KcsA. We therefore decided to characterize the precipitation behavior in more detail, focusing on (a) the role of general hydrophobicity in precipitating DsbB, (b) the nature of the precipitated state, (c) the mechanism of precipitation, and (d) the generality of this behavior.

We repeated the titration of DsbB using the alcohols methanol (MeOH), ethanol (EtOH), *n*-propyl alcohol (PrOH), isopropyl alcohol (iPrOH), and hexafluoroisopropyl alcohol (HFIP) (listed according to increasing hydrophobicity). In all cases, we saw a characteristic decrease in supernatant fluorescence at relatively low alcohol concentrations. Except for MeOH, which is the least hydrophobic of all the solvents tested, this was always followed by a rise in fluorescence to levels approaching (or in PrOH's case exceeding) that of the native state (Figure 1C). Let us define $[Ppt]^{50\%}$ as the alcohol concentration at which the protein is halfway to the minimal fluorescence level starting from the alcohol-free level; this value can be obtained for each alcohol by simple interpolation. Provided we exclude data for HFIP, Figure 1D shows a clear linear relationship between log $[Ppt]^{50\%}$ and alcohol hydrophobicity [defined by their partitioning between water and octanol (*47*)]. This is similar to the observations made for membrane-embedded KcsA (*34*). However, the slope of the plot for DsbB (-1.53 ± 0.15) is significantly higher than that seen for KcsA using the same hydrophobicity values (slope estimated by us to be around -0.67) (*34*).

Let us similarly define $[\text{resolubilization}]^{50\%}$ as the alcohol concentration where the protein is halfway to the highest fluorescence level attained at high alcohol concentration. If the interactions responsible for precipitation and resolubilization are similar in nature, we would expect this parameter to correlate with $[Ppt]^{50\%}$. There is a reasonable linear relationship between the two 50% values (Figure 1D insert), although this may not be significant as the points cluster in one group with a single outlier. The variation in the 335/350 nm ratio with alcohol concentration (Figure 1E) shows a strong correlation with the fluorescence emission intensities: the ratio stays constant until the protein starts to resolubilize, reinforcing the conclusion made from the TFE and activity data that the soluble fraction of the protein remains native-like until it enters the resolubilization range.

As an alternative to alcohol hydrophobicity, we replotted the data in Figure 1C versus the relative dielectric constant ϵ_r of the alcohol−water mixtures, using data from ref *48* to convert concentration to ϵ_r. We see a convergence but not complete coalescence for data between the different alcohols (Figure 1F), suggesting that simple reduction in solvent polarity cannot explain our observations entirely. In particular, it is clear that the resolubilization step differs greatly among alcohols under conditions of comparable polarity.

Aggregation Is Initiated by a Dimerization Reaction. We noted that the final appearance of the titration profile of DsbB in TFE was attained very quickly; overnight incubation did not alter the fluorescence emission levels in the supernatant (data not shown). This indicated that the aggregative processes happened very quickly. We therefore performed stopped-flow experiments to follow the process in more detail, using apparent Trp fluorescence as a sensitive measure of aggregation (similar effects were seen by absorbance changes at 400 nm, but the signal-to-noise ratio was lower). When DsbB is transferred into TFE, there is a lag phase of a few seconds before the (apparent) fluorescence levels rise to a plateau level (Figure 2A). The length of the lag phase is inversely correlated to protein concentration (Figure 2B). In a log−log plot, there is a good linear relationship with a slope of -1.01 ± 0.09. If aggregation is assumed to involve a preequilibrium corresponding to the formation of an oligomeric nucleus, followed by irreversible polymerization, then the first derivative in this log−log plot equals $-n^*/2$, where n^* is the nucleus size (*49*). Our data thus suggest that dimerization is the first step in the aggregation process.

Intermediate Alcohol Concentrations Reduce Membrane Protein Stability. It was of interest to analyze the stability of DsbB at low alcohol concentrations, where a significant fraction of the protein remains soluble and native-like, to see how stability may be coupled to the precipitation process. Thermal stability of DsbB may be monitored via the change in ellipticity at 220 nm (*16*), which provides the midpoint temperature of denaturation t_m. Although DsbB starts to precipitate at the higher end of the alcohol concentration range in these scans, the soluble fraction of DsbB whose stability could be measured by CD-based thermal scanning retained a native far-UV CD spectrum (data not shown). This correlates well with the observation that the 335/350 nm fluorescence emission ratio of the soluble fraction remains roughly constant up to 20% TFE (Figure 1A). Scans at increasing concentrations of different alcohols reveal a linear decline in t_m with alcohol concentration over a restricted concentration range (Figure 3A) (we were unable to obtain satisfactory thermal scans in HFIP). Using the slope of this decline as a measure of the destabilizing influence of the alcohol, we obtain a monotonic and slightly curved relationship with hydrophobicity, which illustrates the clear correlation between increased hydrophobicity and increased destabilizing propensities (Figure 3B). Alternatively, we can estimate the alcohol concentration required to decrease the melting temperature by 10 °C and plot this concentration versus hydrophobicity (Figure 3B). Remarkably, this gives

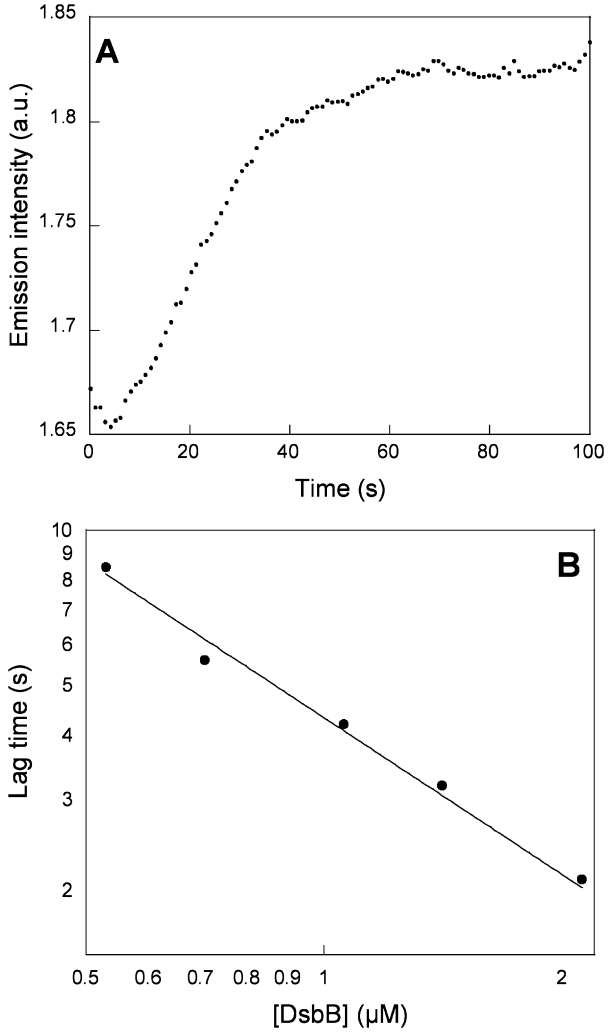

FIGURE 2: (A) Time profile of aggregation of DsbB upon transfer from 0 to 20% TFE. The process was followed by the apparent change in fluorescence, but the magnitude of the signal indicates that significant light scattering is occurring. The lag time t_{lag} is estimated by the intersection of the lag region and the growth region as indicated. (B) Lag time of aggregation as a function of DsbB concentration. The slope of the fitted straight line in the log−log plot is -1.01 ± 0.09.

a linear correlation in a log−log plot with a slope of -1.49 ± 0.17, identical within error to the slope for the precipitation concentrations (Figure 1D). In both cases the slopes show a correlation with hydrophobicity which is significant at the 99% level. This indicates that stability and precipitation are very closely related.

The same relationship between t_m and alcohol concentration was seen when the detergent DM was replaced with octaethylene glycol mono-*n*-dodecyl ether, illustrating that the nature of the detergent is not central in the effect of the alcohol on protein stability (Figure 3C).

The α-Helical Membrane Protein NhaA, but Not the β-Barrel Membrane Protein AIDA, Follows the Same Two-Step Change in Alcohols. To test the generality of alcohols' ability to induce this characteristic sequence of precipitation in membrane proteins, we also tested the behavior of the 388-residue sodium−hydrogen antiporter NhaA, a 12-transmembrane α-helix protein (*38*) which is considerably larger than DsbB. The same general behavior is seen, in which fluorescence decreased sharply at relatively low alcohol

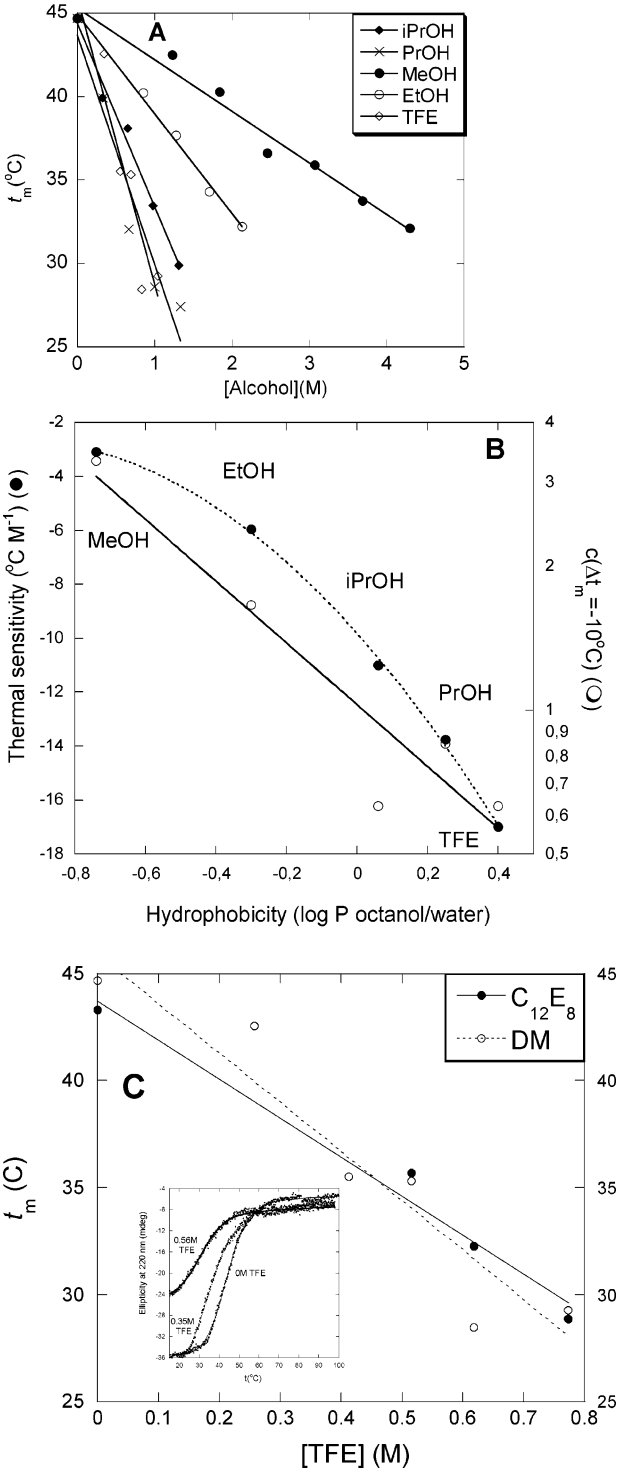

FIGURE 3: (A) Melting temperature t_m of DsbB as a function of different alcohol concentrations. The straight lines represent the best linear fits to the data. (B) The slopes of the fits in (A), and the alcohol concentration required for a 10 °C drop in thermal stability, plotted versus alcohol hydrophobicity. The stippled line is a polynomium intended to guide the eye through the plot of the slope−hydrophobicity data, while the line is the best linear fit of the 10 °C hydrophobicity data. The line has a slope of -1.49 ± 0.17, identical within error to the linear plots in Figure 1D. (C) Change in t_m of DsbB as a function of TFE in two different detergents, namely, DM and $C_{12}E_8$. Insert: Thermal scans for DsbB in 0−0.56 M TFE in the presence of $C_{12}E_8$.

concentrations, followed by a recovery (in the case of PrOH, iPrOH, EtOH, and to some extent TFE) at higher alcohol concentrations (Figure 4A). NhaA solubility increases in

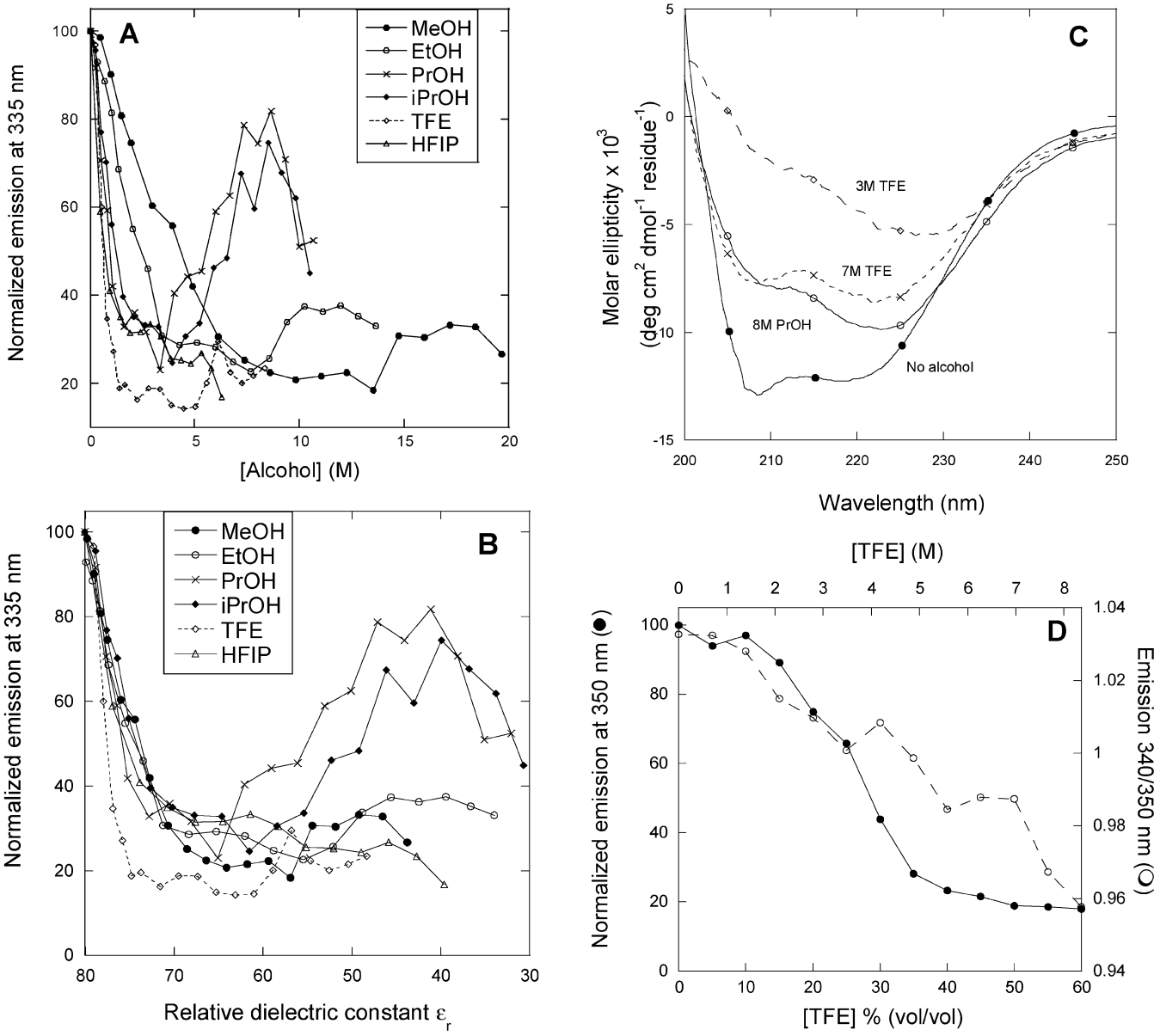

FIGURE 4: (A) Fluorescence emission intensity of NhaA in different alcohols. Emission corresponds closely to solubility (cf. data for TFE in Figure 1B). (B) Data in (A) plotted versus relative dielectric constant ϵ_r rather than alcohol concentration. Concentrations were converted to ϵ_r values based on data in ref *48*. (C) Far-UV CD spectra of NhaA in the native state (no alcohol), the precipitated state (2.8 M TFE), and the resolubilized state (7 M TFE or 8 M PrOH). (D) Emission intensity and emission ratio for the outer membrane β-barrel protein AIDA as a function of TFE concentration.

parallel (Figure 1B). Again, we observe a linear relationship between $[Ppt]^{50\%}$ and alcohol hydrophobicity in a log−log plot when HFIP is excluded, and the slope (-1.58 ± 0.05) is identical within error to that of DsbB (Figure 1D). In the case of NhaA, there is a very marked coalescence of data from different alcohols in the precipitation region when fluorescence data were plotted versus ϵ_r (Figure 4B). There is more divergence in the resolubilization region. Unlike DsbB, NhaA does not show an increase in α-helicity at higher TFE concentrations; according to CD, the α-helical content actually decreases from 41% in 0 M alcohol to 31% in 7 M TFE (Figure 4C). This could partially be due to small light scattering artifacts, since the solution showed a slight opacity in 7 M TFE (data not shown). However, the spectrum in 8 M PrOH (where no opacity is observed) is similar to that in 7 M TFE, although it was not possible to deconvolute it (Figure 4C). Although NhaA only has a slightly higher proportion of transmembrane residues than DsbB [255 residues, corresponding to 66% (*38*)], the residues exposed to the extramembraneous environment are predominantly restricted to form turns between helices and so are presumably less amenable to change to α-helical structures in TFE.

In contrast to the two α-helix membrane proteins DsbB and NhaA, the β-barrel outer membrane protein AIDA (*17*) failed to show any visible precipitation at any TFE concentration with essentially identical fluorescence intensities before and after centrifugation (Figure 4D). Although there was a clear decrease in fluorescence, the linear decline in the 340/350 nm ratio suggested a noncooperative structural transition (Figure 4D).

The Structure of the Precipitated State. It was not feasible to obtain reliable structural information on the aggregates from CD spectra due to excessive light scattering artifacts. However, FTIR is insensitive to the physical state of the

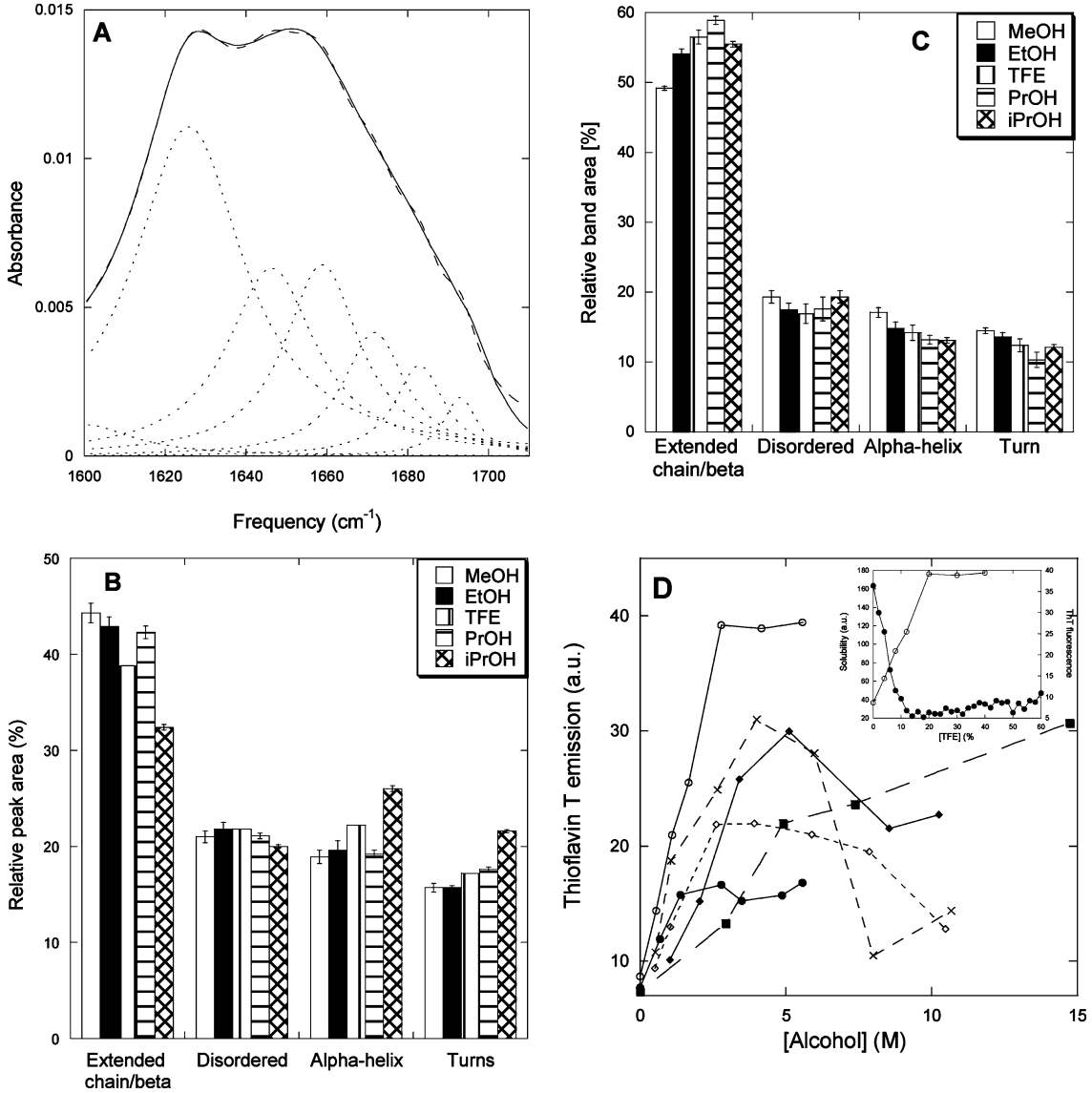

FIGURE 5: (A) FTIR spectrum of DsbB precipitated in 20% (2.8 M) TFE. The stippled lines indicate the deconvoluted peaks assigned to secondary structure elements. (B) Distribution of different secondary structural elements in precipitates of DsbB formed in alcohol concentrations corresponding to lowest solubility (Figure 1A), namely, 2.8 M TFE, 2 M PrOH, 2 M iPrOH, 6 M EtOH, or 15 M MeOH. (C) As in (B) for NhaA in 2.8 M TFE, 15 M MeOH, 6.8 M EtOH, 4.4 M PrOH, or 4 M iPrOH. (D) Thioflavin T fluorescence in the presence of precipitates formed upon incubation of DsbB in (●) TFE and NhaA in (○) TFE, (×) PrOH, (◇) iPrOH, (◆) EtOH, and (■) MeOH at different concentrations. Insert: Correlation between NhaA solubility (●) and ThT fluorescence (○) as a function of TFE concentration.

sample and provides a useful method to characterize these aggregates. Spectra of the DsbB precipitates were recorded at alcohol concentrations where precipitation was maximal. For all alcohols, a clear contribution is observed in the lower β region of the amide I band (Figure 5A). The deconvoluted spectra and the second derivatives showed six contributions for the secondary structure at similar frequencies. A seventh low-intensity Lorentzian peak was added to the fit to account for the contribution of side chains in the lower range of the band. The fitted peaks were centered at 1627 ± 0.2 cm^{-1} (extended chain/β-sheet), 1646 ± 1.0 cm^{-1} (disordered structure), 1659 ± 0.9 cm^{-1} (α-helix), 1672 ± 1.2 and 1684 ± 1.1 cm^{-1} (β turns), and 1694 ± 1.0 cm^{-1} (β-sheet). In all alcohols, the β-sheet structure clearly dominated at the expense of α-helicity. iPrOH showed slightly less β-sheet structure than the other alcohols, with a corresponding increase in the α-helix content as well as β-turns (Figure 5B).

Similar experiments performed for NhaA showed the β-sheet structure to assume an even more dominating role (Figure 5C), with up to 60% β-sheet as opposed to only 40−45% for DsbB.

The increase in β-sheet structure upon incubation at intermediate TFE concentrations raised the question whether the aggregates contained an organized fibrillar structure as seen for water-soluble proteins such as acylphosphatase incubated at 20−30% (2.8−3.8 M) TFE (*32*) and the K3 peptide at 20% TFE (*50*). We therefore incubated samples of DsbB and NhaA at 0.04 mg/mL (i.e., 1.9 μM DsbB or 1 μM NhaA) with TFE for several days, spun down the pellet, and resuspended it in buffer containing the dye thioflavin T (ThT). This dye is known to bind amyloid structures with reasonable specificity (*51*). For both proteins, a significant rise in the ThT signal was observed in the concentration range where DsbB and NhaA precipitate (Figure 5C and insert), although the increase was higher for NhaA. A similar

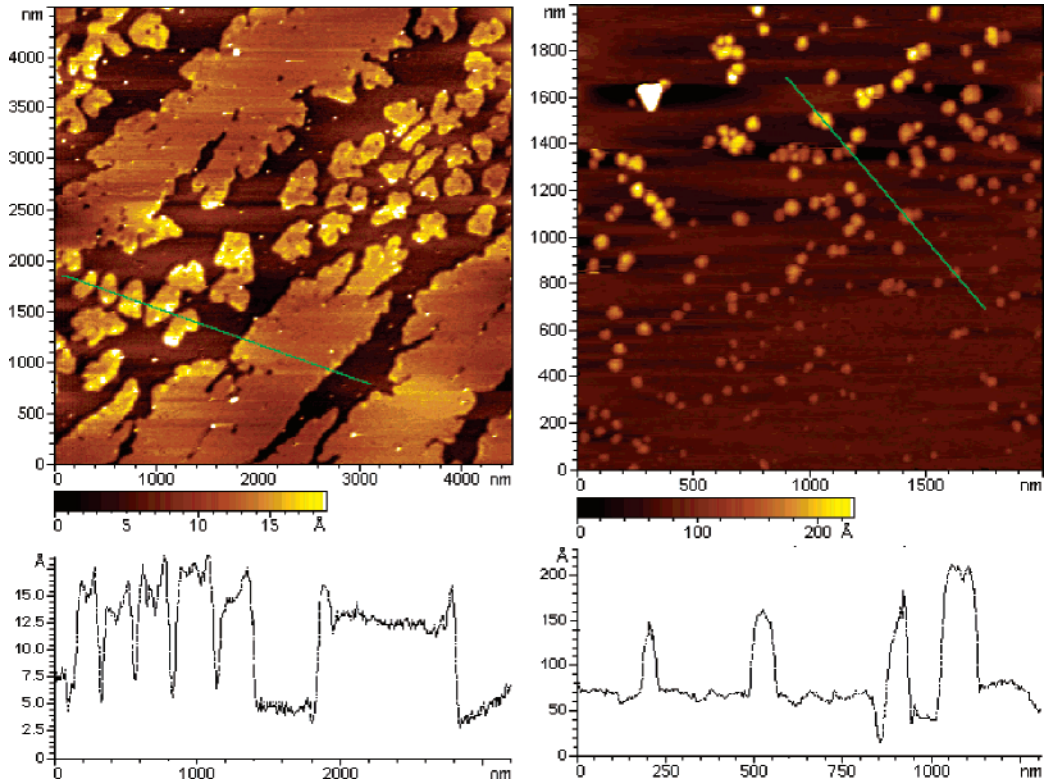

FIGURE 6: Atomic force microscopy images of NhaA precipitates formed in the presence of 2.8 M TFE. The bottom panels display the height profile of the green lines in the AFM images.

analysis of NhaA's structure in other alcohols revealed the same general behavior, in which the ThT signal increases in parallel with the amount of precipitated protein and then declines at high concentrations where the protein becomes resolubilized (Figure 5D).

Nevertheless, the increase in ThT signal is not unequivocal evidence for fibril formation. ThT is also able to bind to nonfibrillar structures, ranging from the acetylcholinerase receptor (*52*) to amorphous aggregates (D. E. Otzen, unpublished observations). Most fibrillation reactions proceed over hours to days and are preceded by a lag time during which nuclei can form (*53*). However, the kinetics of formation of these ThT-positive structures is rapid and the ThT fluorescence level stabilizes within at most 30 min; no further change is seen upon incubation for several days (data not shown). Stronger evidence for the lack of fibrillated aggregates was provided by the amyloid-specific chromophore Congo Red, which did not undergo any spectral change in the presence of these aggregates (data not shown). We used atomic force microscopy to visualize the aggregates of NhaA formed in 2.8M TFE. Much of the mica surface was covered by a layer of a uniform depth of approximately 10 Å (Figure 6A) which coexisted with circular aggregates of varying sizes that were up to 100 Å tall (Figure 6B), indicating a variety of different aggregate structures. However, no bona fide fibrils were observed.

DISCUSSION

We initially hoped to find means of reversibly denaturing monomeric MPs in alcohols as an alternative to detergent solubilization. While alcohols are very useful for reversible dissociation of oligomeric complexes (*36*), it has not been investigated in detail how they affect monomeric membrane proteins. The aim was to be able to obtain reliable estimates of membrane protein stability under conditions where the denatured state is truly denatured and not just a slightly expanded version of the native state, as has been suggested to be the case for the SDS-denatured state (*20*). For the two α-helical MPs tested here, we find no cooperative unfolding in traditional chemical denaturants. In view of recent reports on the ability of the fluorinated alcohol TFE to reversibly denature the membrane protein KcsA at intermediate concentrations (*36*), we therefore decided to systematically test several fluorinated and nonfluorinated alcohols for their ability to induce reversible conformational changes. We find that both proteins irreversibly precipitate at intermediate concentrations of alcohol, and although they are solubilized at higher concentrations of alcohol, dilution does not restore activity. Resolubilization only occurs because the protein is forced into a non-native state which can be more effectively solubilized. These experiments all had to be done in the presence of detergents, since their absence would only make precipitation more pronounced. Thus, increasing detergent concentration simply postponed precipitation to higher alcohol concentrations. We therefore conclude that alcohols, fluorinated or not, do not provide a useful general means of inducing reversible unfolding of membrane proteins in solution. Nevertheless, the conformational changes induced by these alcohols are worthy of further comments.

Precipitation through Destabilization and Structural Frustration. Let us start by focusing on the precipitation occurring at low to medium alcohol concentrations. Cosmotropic salts, such as sodium sulfate, precipitate proteins by hyperstabilizing them; they are preferentially excluded from the protein surface (*54*) and thus favor compact conformations with minimized exclusion zones. At lower salt concentrations, this

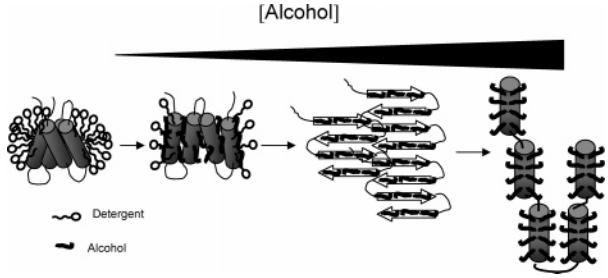

FIGURE 7: Proposed model for alcohol-induced destabilization, precipitation, and resolubilization of membrane proteins. Alcohol molecules may disrupt helix−helix contacts and displace detergent molecules, leading eventually to destabilization and precipitation to β-rich structures, until sufficiently high alcohol concentrations disrupt the β-sheet structure and lead to non-native predominantly α-helical (DsbB) or other non-native (NhaA) states.

will lead to a significant stabilization of the native state relative to the denatured state (*55*), whereas higher salt concentrations eventually induce precipitation of the native state so as to minimize contact with solvent. The alcohols precipitate membrane proteins by a mechanism which is fundamentally different from this. Thermal scans with DsbB indicate that destabilization of the native state of the protein is a prelude to precipitation.

On the basis of this, we speculate that the alcohols are able to bind to hydrophobic parts of the membrane protein via their aliphatic groups, both on the surface-exposed parts of the protein, which are normally sequestered by detergents, and internally in the protein, disrupting tertiary helix−helix contacts which are important stabilizing elements. This will lead to structural frustration, since the alcohol disturbs the normal protein−protein and protein−detergent contacts which maintain the protein in a solubilized native state, while being unable to provide a sufficiently effective solvent to keep the protein in solution (Figure 7). This is corroborated by several observations: First, the good correlation between $[Ppt]^{50\%}$ and hydrophobicity (Figure 1F) is evidence that the more hydrophobic the alcohol, the higher affinity it has for the hydrophobic patches on the protein. In addition, alcohol hydrophobicity is linked to precipitation and destabilization parameters by exactly the same slope (Figures 1D and 3A). Second, the precipitation data for different alcohols converge when plotted versus dielectric constant rather than molar concentration, indicating that exposure of otherwise sequestered parts of membrane proteins to solvents with high polarity will of necessity lead to precipitation. The convergence is particularly clear for NhaA, which has a larger proportion of transmembrane residues than DsbB and is therefore a "cleaner" membrane protein. For water-soluble proteins, where solubility is not such a sensitive issue, the protein will typically respond to changes in ϵ_r by undergoing conformational transitions at the monomeric level (*48*, *56*). Third, the low fraction of the protein population that remains in solution at intermediate alcohol concentrations has native-like fluorescence emission ratios (Figure 1), suggesting that adoption of the non-native conformation induced by alcohols is not compatible with staying in solution. Fourth, the β-barrel membrane protein AIDA remains solubilized throughout the same alcohol concentration range that leads to massive precipitation of DsbB and NhaA, supporting the fact that the tertiary structure of helical membrane proteins is predominantly stabilized by strongly hydrophobic contacts between transmembrane helices that can be disrupted by the alcohols (*2*, *3*). β-Barrel membrane proteins consist of amphiphilic sequences which do not provide such suitable binding sites. In addition to direct alcohol−protein interactions, it could also be expected that the more hydrophobic alcohols more strongly partition into the protein−detergent complex. This could conceivably lead to early disruption of micelles and subsequent precipitation. However, the fact that AIDA, which also requires micellar detergent to stay in solution (*41*), remains solubilized throughout the titration argues that there is little actual stripping of detergents off the membrane protein surface.

Rapid Formation of Stable but Nonfibrillar Precipitates Driven by Hydrophobic Effects. The structural frustration induced by the alcohols leads to very rapid (second-scale) precipitation, driven by the hydrophobic effect. It is a well-defined process with a discernible lag phase where the rate-limiting step is the formation of dimers. This leads to the formation of thioflavin T-positive β-rich precipitates with organized but nonfibrillar structure that also shows great variations in height, indicating a heterogeneous population of aggregates (Figure 6). Thus, under these conditions, formation of intermolecular β-sheet structures is the most effective way of satisfying hydrogen-bonding requirements. Aggregation at intermediate TFE concentrations (peaking at 25%) is also seen for water-soluble proteins such as acylphosphatase (*32*) and the K3 peptide from β_2-microglobulin (*50*). For AcP, aggregation initially leads to the formation of relatively amorphous aggregates which only form ordered structures over a time scale of many days (*57*). No such transitions were observed upon longer term exposure of DsbB and NhaA. Presumably, the strong hydrophobic interactions between the membrane protein molecules effectively trap the precipitated state in a stable conformation which cannot rearrange to other structures. This contrasts with strongly fibrillating peptides such as the 42-residue Alzheimer Aβ peptide, whose C-terminal domain is a fragment of a membrane-spanning helix while the N-terminus is hydrophilic. Similarly, truncation of the transmembrane-spanning part of glycophorin, making it unable to span the membrane bilayer, induces fibrillation within a few days (*58*). The key to their fibrillation propensity, in contrast to full-length membrane proteins, probably lies in (a) their relatively small size, making conformational changes more accessible, and (b) a disruption (truncation) of the normal hydrophobic interactions at a very fundamental level.

Resolubilization Follows Alcohol-Specific Patterns. As we increase the alcohol concentration, it becomes possible to resolubilize the β-rich precipitates to structures rich in α-helicity but with altered tertiary structure, as witnessed by the change in the 335/350 nm emission (Figure 1). In contrast to the alcohols' general ability to precipitate DsbB and NhaA at low concentrations, resolubilization does not follow a simple pattern. To some extent, resolubilization depends on hydrophobicity: the weakly hydrophobic alcohol MeOH cannot resolubilize the precipitates, unlike EtOH, PrOH, iPrOH, and TFE. MeOH, as opposed to other alcohols, has also been shown to induce β-rich structures in the all-helical protein VlsE (*33*) and the α/β protein ervatamin (*59*). However, plotting precipitation data versus ϵ_r (Figure 1D) clearly reveals that changes in ϵ_r cannot explain the resolubilization. In the same ϵ_r range where PrOH, iPrOH, TFE,

and EtOH achieve high solubilization (but starting at different values of ϵ_r), neither MeOH nor HFIP shows any effect. The fluorinated alcohol TFE does not distinguish itself from the nonfluorinated alcohols in precipitation and resolubilization, suggesting that the fluorinated groups do not play any specific role in these phenomena. However, the "hyperfluorinated" alcohol HFIP is not as potent a denaturant as would be predicted from its hydrophobicity. For example, it does not decrease $[Ppt]^{50\%}$ for DsbB and NhaA as much as expected and does not show strong resolubilization properties. The basis for this decreased potency could be related to the inability of fluorine groups in hemifluorinated surfactants to mix with lipids (*60*). On the other hand, HFIP conforms to the general hydrophobicity-driven ability of alcohols to dissociate KcsA tetramers in lipid membranes (*34*). Thus resolubilization appears to be more sensitive to the nature of the alcohol than precipitation, possibly because the alcohol molecules have to bind well to the hydrophobic surfaces to shield the protein against aggregation.

A thought-provoking study on the effect of alcohols on the conformational transitions of the aggregation-prone protein α-synuclein revealed that nonfluorinated alcohols led to β-rich oligomer formation, while HFIP and TFE led to α-rich monomers (*26*). The authors suggested that MeOH and EtOH mimic the environment near the membrane, and TFE and HFIP mimic the environment *in* the membrane, simply because TFE and HFIP are more hydrophobic. These considerations are likely to apply for water-soluble proteins. However, for membrane proteins, which are unequivocally dependent on a membrane-like environment, TFE and HFIP are clearly not sufficiently membrane-like to keep the membrane protein in solution.

TFE and HFIP have also been shown to form higher order clusters at concentrations around 15−65% (v/v) (*48*). However, these clusters cannot be instrumental in resolubilization. TFE only solubilizes DsbB from around 35% onward, whereas HFIP, which has a much greater propensity to form these clusters, does not resolubilize to any significant extent, and the nonclustering alcohol EtOH solubilizes just as efficiently as TFE.

In conclusion, we have shown that alcohols can induce numerous conformational changes in membrane proteins, leading to destabilization, precipitation, and resolubilization. Destabilization and precipitation correlate well with hydrophobicity, whereas resolubilization also involves effects specific for each alcohol. These phenomena highlight the fact that alcohols can exert an effect on membrane proteins, not just by modulating the actual lipid environment (*34*) but also by directly affecting the intrinsic stability of the membrane protein. The effect on membrane protein stability is comparable to the effect on lateral pressure, since the change in the midpoint of precipitation of NhaA and DsbB is more than twice as sensitive to alcohol hydrophobicity as the dissociation midpoints for the KcsA tetramer.

REFERENCES

1. Popot, J.-L., and Engelman, D. M. (1990) Membrane protein folding and oligomerization: the two-stage model, *Biochemistry 29*, 4031−4037.
2. Popot, J. L., and Engelman, D. M. (2000) Helical membrane protein folding, stability, and evolution, *Annu. Rev. Biochem. 69*, 881−922.
3. Stowell, M. H. B., and Rees, D. C. (1995) Structure and stability of membrane proteins, *Adv. Protein Chem. 46*, 279−311.
4. Wimley, W. C. (2002) Toward genomic identification of beta-barrel membrane proteins: composition and architecture of known structures, *Protein Sci. 11*, 301−312.
5. Jähnig, F., and Surrey, T. (1997) Folding and insertion of proteins into membranes in vitro, in *Membrane Protein Assembly* (Von Heijne, G., Ed.) pp 83−98, R. G. Landes Co., Heidelberg, Germany.
6. Kleinschmidt, J. H., and Tamm, L. K. (1996) Folding intermediates of a beta-barrel membrane protein. Kinetic evidence for a multi-step membrane insertion mechanism, *Biochemistry 35*, 12993−13000.
7. Hong, H., and Tamm, L. K. (2004) Elastic coupling of integral membrane protein stability to lipid bilayer forces, *Proc. Natl. Acad. Sci. U.S.A. 101*, 4065−4070.
8. Booth, P. J., Flitsch, S. L., Stern, L. J., Greenhalgh, D. A., Kim, P. S., and Khorana, H. G. (1995) Intermediates in the folding of the membrane protein bacteriorhodopsin, *Nat. Struct. Biol. 2*, 139−143.
9. Faham, S., Yang, D., Bare, E., Yohannan, S., Whitelegge, J. P., and Bowie, J. U. (2004) Side-chain contributions to membrane protein structure and stability, *J. Mol. Biol. 335*, 297−305.
10. Lau, F. W., and Bowie, J. U. (1997) A method for assessing the stability of a membrane protein, *Biochemistry 36*, 5884−5892.
11. Otzen, D. E. (2003) Folding of DsbB in mixed micelles: A kinetic analysis of the stability of a bacterial membrane protein, *J. Mol. Biol. 330*, 641−649.
12. Reynolds, J. A., and Tanford, C. (1970) The gross conformation of protein-sodium dodecyl sulfate complexes, *J. Biol. Chem. 245*, 5161−5165.
13. Tanford, C. (1980) *The Hydrophobic Effect. Formation of Micelles and Biological Membranes*, 2nd ed., Wiley & Sons, New York.
14. Turro, N. J., Lei, X.-G., Ananthapadmanabhan, K. P., and Aronson, M. (1995) Spectroscopic probe analysis of protein-surfactant interactions: the BSA/SDS system, *Langmuir 11*, 2525−2533.
15. Ibel, K., May, R. P., Kirschner, K., Szadkowski, H., Mascher, E., and Lundahl, P. (1990) Protein-decorated micelle structure of sodium-dodecyl-sulfate-protein complexes as determined by neutron scattering, *Eur. J. Biochem. 190*, 311−318.
16. Sehgal, P., and Otzen, D. E. (2006) Thermodynamics of unfolding of an integral membrane protein in mixed micelles, *Protein Sci. 15*, 890−899.
17. Sehgal, P., Mogensen, J. E., and Otzen, D. E. (2005) Using micellar mole fractions to assess membrane protein stability in mixed micelles, *Biochim. Biophys. Acta 1716*, 59−68.
18. Riley, M. L., Wallance, B. A., Flitsch, S. L., and Booth, P. J. (1997) Slow alpha helix formation during folding of a membrane protein, *Biochemistry 36*, 192−196.
19. Woolhead, C. A., McCormick, P. J., and Johnson, A. E. (2004) Nascent membrane and secretory proteins differ in FRET-detected folding far inside the ribosome and in their exposure to ribosomal proteins, *Cell 116*, 725−736.
20. Renthal, R., and Alloor, S. R. (2006) Partially unfolded membrane protein has a compact conformation, *FASEB J. 20* (in press).
21. Renthal, R. (2006) An unfolding story of helical transmembrane proteins, *Biochemistry 45*, 14559−14566.
22. Wilkinson, K. D., and Mayer, A. N. (1986) Alcohol-induced conformational changes of ubiquitin, *Arch. Biochem. Biophys. 250*, 390−399.
23. Dufour, E., Bertrand-Harb, C., and Haertlé, T. (1993) Reversible effects of medium dielectric constant on structural transformation of beta-lactoglobulin and its retinol binding, *Biopolymers 33*, 589−598.
24. Bychkova, V. E., Dujsekina, A. E., Klenin, S. I., Tiktopulo, E. I., Uversky, V. N., and Ptitsyn, O. B. (1996) Molten globule-like state of cytochrome *c* under conditions simulating those near the membrane surface, *Biochemistry 35*, 6058−6063.
25. Buck, M. (1998) Trifluoroethanol and colleagues: cosolvents come of age. Recent studies with peptides and proteins, *Q. Rev. Biophys. 31*, 297−355.
26. Munishkina, L. A., Phelan, C., Uversky, V. N., and Fink, A. L. (2003) Conformational behaviour and aggregation of alpha-synuclein in organic solvents: modeling the effects of membranes, *Biochemistry 42*, 2720−2730.

27. Dzwolak, W., Grudzielanek, S., Smirnovas, V., Ravindra, R., Nocilini, C., Jansen, R., Loksztejn, A., Porowski, S., and Winter, R. (2005) Ethanol-perturbed amyloidogenic self-assembly of insulin: Looking for origins of amyloid strains, *Biochemistry 44*, 8948−8958.
28. Kamatari, Y. O., Konno, T., Kataoka, M., and Akasaka, K. (1998) The methanol-induced transition and the expanded helical conformation in hen lysozyme, *Protein Sci. 8*, 873−882.
29. Shiraki, K., Nishikawa, K., and Goto, Y. (1995) Trifluoroethanol-induced stabilisation of the alfa-helical structure of β-lactoglobulin: Implication for non-hirarchial protein folding, *J. Mol. Biol. 245*, 180−194.
30. Hirota, N., Mizuno, K., and Goto, Y. (1998) Group additive contributions to the alcohol-induced alpha-helix formation of melittin: Implication for the mechanism of the alcohol effects on proteins, *J. Mol. Biol. 275*, 365−378.
31. Jasanoff, A., and Fersht, A. R. (1994) Quantitative determination of helical propensities from trifluoroethanol titration curves, *Biochemistry 33*, 2129−2135.
32. Chiti, F., Taddei, N., Bucciantini, M., White, P., Ramponi, G., and Dobson, C. M. (2000) Mutational analysis of the propensity for amyloid formation by a globular protein, *EMBO J. 19*, 1441−1449.
33. Perham, M., Liao, J., and Wittung-Stafshede, P. (2006) Differential effects of alcohols on conformational switchovers in alpha-helical and beta-sheet protein models, *Biochemistry 45*, 7740−7749.
34. van den Brink-van der Laan, E., Chupin, V., Killian, J. A., and de Kruijff, B. (2004) Small alcohols destabilize the KcsA tetramer via their effect on the membrane lateral pressure, *Biochemistry 43*, 5937−5942.
35. van den Brink-van der Laan, E., Chupin, V., Killian, J. A., and de Kruijff, B. (2004) Stability of KcsA tetramer depends on membrane lateral pressure, *Biochemistry 43*, 4240−4250.
36. Barrera, F. N., Renart, M. L., Molina, M. L., Poveda, J. A., Encinar, J. A., Fernández, A. M., Neira, J. L., and González-Ros, J. M. (2005) Unfolding and refolding in vitro of a tetrameric, alpha-helical membrane protein: The prokaryotic potassium channel KcsA, *Biochemistry 44*, 14344−14352.
37. Spelbrink, R. E. J., Kolkman, Slijper, M., Killian, J. A., and De Kruijff, B. (2005) Detection and identification of stable oligomeric protein complexes in *Escherichia coli* inner membranes: A proteomics approach, *J. Biol. Chem. 280*, 28742−28748.
38. Hunte, C., Screpanti, E., Venturi, M., Rimon, A., Padan, E., and Michel, H. (2005) Structure of a Na^+/H^+ antiporter and insights into mechanism of action and regulation by pH, *Nature 435*, 1197−1202.
39. Otzen, D. E. (2002) Folding of the α-helical membrane proteins DsbB and NhaA, in *Biophysical Chemistry: Membranes and Proteins* (Seddon, J., Ed.) pp 208−214, Royal Society of Chemistry, London.
40. Wunderlich, M., and Glockshuber, R. (1993) Redox properties of protein disulfide isomerase (DsbA) from *Escherichia coli*, *Protein Sci. 2*, 717−726.
41. Mogensen, J. E., Tapadar, D., Schmidt, M. A., and Otzen, D. E. (2005) Barriers to folding of the transmembrane domain of the *Escherichia coli* autotransporter adhesin involved in diffuse adherence, *Biochemistry 44*, 4533−4545.
42. Azab, H. A., El-Nady, A. M., and Saleh, M. S. (1994) Potentiometric determination of the second stage dissociation constant of N-[tris-(hydroxymethyl)-methyl]-2-aminoethane-sulphonic acid (TES) in different solvent mixtures, *Monatsh. Chem. 125*, 233−240.
43. Bader, M., Muse, W., Ballou, D. P., Gassner, C., and Bardwell, J. C. A. (1999) Oxidative protein folding is driven by the electron transport system, *Cell 98*, 217−227.
44. Otzen, D. E., Lundvig, D., Wimmer, R., Hatting, L., Pedersen, J. R., and Jensen, P. H. (2005) p25alpha is flexible but natively folded and binds tubulin in an oligomeric complex, *Protein Sci. 14*, 1396−1409.
45. Andrade, M. A., Chacón, P., Merelo, J. J., and Morán, F. (1993) Evaluation of secondary structure of proteins from UV circular dichroism using an unsupervised learning neural network, *Protein Eng. 6*, 383−390.
46. Jander, G., Martin, N. L., and Beckwith, J. (1994) Two cysteines in each periplasmic domain of the membrane protein DsbB are required for its function in protein disulfide bond formation, *EMBO J. 13*, 5121−5127.
47. Abraham, M. H., Chadha, H. S., Whiting, G. S., and Mitchell, R. C. (1994) Hydrogen bonding. 32. An analysis of water-octanol and water-alkane partitioning and the delta-log P parameter of Seiler, *J. Pharm. Sci. 83*, 1085−1100.
48. Hong, D.-P., Hoshino, M., Kuboi, R., and Goto, Y. (1999) Clustering of fluorine-substituted alcohols as a factor responsible for their marked effects on proteins and peptides, *J. Am. Chem. Soc. 121*, 8427−8433.
49. Goldstein, R. F., and Stryer, L. (1986) Cooperative polymerization reactions. Analytical approximations, numerical examples, and experimental strategy, *Biophys. J. 50*, 583−599.
50. Yamaguchi, K.-I., Naiki, H., and Goto, Y. (2006) Mechanism by which the amyloid-like fibrils of a beta2-microglobulin fragment are induced by fluorine-substituted alcohols, *J. Mol. Biol. 363*, 279−288.
51. Levine, H. I. (1999) Quantification of β-sheet amyloid fibril structures with thioflavin T, *Methods Enzymol. 309*, 274−284.
52. Ferrari, G. V. d., Mallender, W. D., Inestrosa, N. C., and Rosenberry, T. L. (2001) Thioflavin T is a fluorescent probe of the acetylcholinesterase peripheral site that reveals conformational interactions between the peripheral and acylation sites, *J. Biol. Chem. 276*, 23282−23287.
53. Harper, J. D., and Lansbury, P. T. J. (1997) Models of amyloid seeding in Alzheimer's disease and scrapie: mechanistic truths and physiological consequences of the time-dependent solubility of amyloid proteins, *Annu. Rev. Biochem. 66*, 385−407.
54. Timasheff, S. (2002) Protein hydration, thermodynamic binding, and preferential hydration, *Biochemistry 41*, 13473−13482.
55. Parker, M. J., Dempsey, C. E., Lorch, M., and Clarke, A. R. (1997) Acquisition of native beta-strand topology during the rapid collapse phase of protein folding, *Biochemistry 36*, 13396−13405.
56. Uversky, V. N., Narizhneva, N. V., Kirschstein, S. O., Winter, S., and Löber, G. (1997) Conformational transitions provoked by organic solvents in β-lactoglobulin: can a molten globule like intermediate be induced by the decrease in dielectric constant?, *Folding Des. 2*, 163−172.
57. Chiti, F., Webster, P., Taddei, N., Clark, A., Stefani, M., Ramponi, G., and Dobson, C. M. (1999) Designing conditions for *in vitro* formation of amyloid protofilaments and fibrils, *Proc. Natl. Acad. Sci. U.S.A. 96*, 3590−3594.
58. Liu, W., Crocker, E., Zhang, W., Elliott, J. I., Luy, B., Li, H., and Smith, S. O. (2005) Structural role of glycine in amyloid fibrils formed from transmembrane alpha-helices, *Biochemistry 44*, 3591−3597.
59. Sundd, M., Kundu, S., and Jagannadham, M. V. (2000) Alcohol-induced conformational transitions in ervatamin C. An alpha-helix to beta-sheet switchover, *J. Protein Chem. 19*, 169−176.
60. Palchevskyy, S. S., Posokhov, Y. O., Olivier, B., Popot, J. L., Pucci, B., and Ladokhin, A. S. (2006) Chaperoning of insertion of membrane proteins into lipid bilayers by hemifluorinated surfactants: Application to diphtheria toxin, *Biochemistry 45*, 2629−2635.

BI700091R